A bioluminescent mouse model of proliferation to highlight early stages of pancreatic cancer: A suitable tool for preclinical studies

UNIVERSITÀ DEGLI STUDI DI TORINO

A bioluminescent mouse model of proliferation to highlight early stages of pancreatic cancer: a suitable tool for preclinical studies.

de Latouliere Luisa[a], Manni Isabella[a*], Iacobini Carla[b], Pugliese Giuseppe[b], Grazi Gian Luca[c], Perri Pasquale[c], Cappello Paola[de], Novelli Franco[de], Menini Stefano[b], Piaggio Giulia[a*]

[a]Department of Research, Advanced Diagnostics and Technological Innovation, Regina Elena National Cancer Institute; Via Elio Chianesi 53, 00144, Rome, Italy.

[b]Department of Clinical and Molecular Medicine, Sapienza University of Rome, Via di Grottarossa 1035-1039, 00189 Rome, Italy.

[c]Department of Experimental Oncology Regina Elena National Cancer Institute; Via Elio Chianesi 53, 00144, Rome, Italy.

[d]Department of Molecular Biotechnologies and Health Sciences, University of Turin; Via Nizza 52, 10126 Torino, Italy.

[e]Center for Experimental Research and Medical Studies, Città della Salute e della Scienza di Torino, Via Santena 5, 10126 Torino, Italy.

Corresponding authors:
Giulia Piaggio, Regina Elena National Cancer Institute, Via Elio Chianesi 53, 00144-Rome, Italy. Phone:+39-06-5266-2458, Fax:+39-06-4180-526; e-mail: piaggio@ifo.it
Isabella Manni, Regina Elena National Cancer Institute, Via Elio Chianesi 53, 00144-Rome, Italy. Phone:+39-06-5266-2585, Fax:+39-06-4180-526; e-mail: manni@ifo.it

Keywords: pancreatic cancer, disease animal models, comparative pathology, molecular imaging, proliferation

Abbreviations
PDAC: pancreatic ductal adenocarcinoma
KC: *LSL-Kras$^{G12D/+}$; Pdx-1-Cre*
KPC: *LSL-Kras$^{G12D/+}$; LSL-Trp53$^{R172H/+}$; Pdx-1-Cre*
PanIN: Pancreatic Intraepithelial Neoplasia
BLI: bioluminescence imaging

Abstract

Transgenic mouse models designed to recapitulate genetic and pathologic aspects of cancer are useful to study early stages of disease as well as its progression. Among several, two of the most sophisticated models for pancreatic ductal adenocarcinoma (PDAC) are the *LSL-Kras*$^{G12D/+}$*;Pdx-1-Cre* (KC) and *LSL-Kras*$^{G12D/+}$*;LSL-Trp53*$^{R172H/+}$*;Pdx-1-Cre* (KPC) mice, in which the Cre-recombinase regulated by a pancreas–specific promoter activates the expression of oncogenic *Kras* alone or in combination with a mutant *p53*, respectively. Non-invasive *in vivo* imaging offers a novel approach to preclinical studies introducing the possibility to investigate biological events in the *spatio*/temporal dimension. We recently developed a mouse model, *MITO-Luc*, engineered to express the luciferase reporter gene in cells undergoing active proliferation. In this model, proliferation events can be visualized non-invasively by bioluminescence imaging (BLI) in every body district *in vivo*. Here, we describe the development and characterization of *MITO-Luc*-KC- and -KPC mice. In these mice we have now the opportunity to follow PDAC evolution in the living animal in a time frame process. Moreover, by relating *in vivo* and *ex vivo* BLI and histopathological data we provide evidence that these mice could represents a suitable tool for pancreatic cancer preclinical studies. Our data also suggest that aberrant proliferation events take place early in pancreatic carcinogenesis, before tumour appearance.

1 Introduction

Pancreatic ductal adenocarcinoma (PDAC) is incurable, with patients often presenting a metastatic disease resistant to therapy. The disease progresses through pancreatic intraepithelial neoplasia (PanIN) lesions to PDAC. Histologically, PanINs are divided into three stages, PanIN-1A,B, PanIN-2 and PanIN-3, defined by increasing degrees of cellular architectural atypia. PDAC is further characterized by a massive stromal reaction and inflammation. Genetically, activating mutations in *Kras* gene seem to be an ubiquitous event, although mutations in *p53* or other genes are also common (Hidalgo, 2012). Early detection is the key to improving survival in PDAC. However several factors contribute to make harder diagnosis of pancreatic cancer at early stages: the anatomical location of the pancreas, the symptoms that are typically associated with advanced disease and the low resolution of conventional imaging modalities. Thus early detection strategies of sporadic pancreatic cancer are urgently needed.

Genetically engineered mouse models (GEMMs) of cognate human diseases allow the identification of molecular mechanisms of disease pathogenesis (Tuveson et al., 2011). Several GEMMs that accurately mimic the pathophysiological features of human PDAC have been described (Tuveson and Hingorani, 2005; Cappello and Novelli, 2013). In particular, a mouse model (KC), in which a "*lox–stop–lox*" $Kras^{G12D}$ allele is expressed in murine pancreatic progenitor cells using a pancreas-specific Cre recombinase and that recapitulates all human features developing both preneoplastic and invasive PDAC, has been characterized (Hingorani et al., 2003). Moreover, in a mouse model that incorporate a *p53* mutation corresponding to the $Trp53^{R172H}$ hotspot mutation in human cancers (KPC), it has been demonstrated that the expression of an endogenous $Kras^{G12D}$ allele cooperates with that of a concomitant *p53* mutation to closely recapitulate the human disease at the pathophysiological and molecular level showing accelerated disease onset and metastasis (Hingorani et al., 2005). Although these models have been useful for therapeutic vaccination and pharmacological treatment in several preclinical studies (Cappello et

al., 2013; Cappello and Novelli 2013; Capello et al., 2013), the current methodological approaches are static and restrict the analysis to a specific phase of tumorigenesis or to a particular snapshot of time, therefore, they do not provide a dynamic view of carcinogenesis useful to identify early steps for which the environment is compulsory for tumour progression.

Non-invasive bioluminescence imaging (BLI) is a powerful tool to study molecular events over time in a living organism (Signore et al., 2010). When combined with cancer models, this technology gives an unprecedented opportunity to investigate molecular events resulting in neoplastic development and progression in the entire organism We have recently developed a reporter mouse model, the *rep*TOP^{TM} *mito*IRE (*MITO-Luc*), in which it is possible to measure physiological and/or aberrant proliferation in any body tissue by BLI (Goeman et al., 2012; Spallotta et al., 2013; Oliva et al., 2013; Rizzi et al., 2015). In these mice the transcription of the firefly luciferase reporter gene is selectively induced during the cell cycle by the transcription factor NF-Y, a trimeric transcription activator composed of NF-YA, NF-YB, and NF-YC subunits, all required for DNA binding. The NF-Y complex exerts its activity only in proliferating cells regulating basal transcription of regulatory genes responsible for cell cycle progression (Farina et al., 1999; Manni et al., 2001; Sciortino et al., 2001; Gurtner et al., 2003; Di Agostino et al., 2006; Gurtner et al., 2008; Manni et al., 2008; Gurtner et al., 2010).

Deregulation of cell cycle and consequent aberrant proliferation have been implicated in the early steps of the carcinogenic process, including PDAC (Hezel et al., 2006). Thus, we hypothesized that the visualization of hyperproliferation occurring during early carcinogenesis could allow us to identify the first stages of tumour development. Based on this hypothesis we crossed KC and KPC mice, in which the somatic activation of *Kras*^{G12D} (KC) and mutant *Trp53*^{R172H} (KPC) is mediated by *Pdx-1-Cre* (Hingorani et al., 2003; Hingorani et al., 2005), with *Mito-Luc* mice (Goeman et al., 2012) generating MKC and MKPC mouse models. By correlating BLI and histopathological analysis of the pancreas from these mice we provide evidence that we are able to follow tumour evolution in terms of cell proliferation in a time frame manner. Of note, we

have identified early steps of pancreatic carcinogenesis thus making these models useful for preclinical pharmacological studies.

2 Material and methods

2.1 Mouse Strains

All animal studies were approved by the Institutional Animal Care of the Regina Elena National Cancer Institute and by the Government Committee of National Minister of Health and were conducted according with EU Directive 2010/63/EU for animal experiments http://ec.europa.eu/environment/chemicals/lab_animals/legislation_en.htm

LSL-Kras$^{G12D/+}$;LSL-Trp53$^{R172H/+}$ mice and *Pdx-1-Cre* transgenic mice (Hingorani et al., 2003; Hingorani et al., 2005) were interbred with *MITO-Luc* reporter mice (Goeman et al., 2012) to obtain *MITO;LSL-Kras$^{G12D/+}$;Pdx-1-Cre* and *MITO;LSL-Kras$^{G12D/+}$;LSL-Trp53$^{R172H/+}$;Pdx-1-Cre*, respectively. The *LSL-Kras$^{G12D/+}$* and *LSL-Trp53$^{R172H/+}$* lineages were maintained in the heterozygous state.

2.2 Genotyping of transgenic mice

After genomic DNA extraction of tail biopsies, the positive founder animals were identified by PCR using the following primers specific for the transgenes:

MITO: oligonucleotide up: 5′-TGTAGACAAGGAAACAACAAAGCCTGGTGGCC;
oligonucleotide down: 5′-GGCGTCTTCCATTTTACCAACAGTACCGG.

Kras: oligonucleotide 1: 5′-GTCTTTCCCCAGCACAGTGC;
oligonucleotide 2: 5′-CTCTTGCCTACGCCACCAGCTC;
oligonucleotide 3: 5′-AGCTAGCCACCATGGCTTGAGTAAGTCTGCA.

Trp53: oligonucleotide 1: 5′-AGCTAGCCACCATGGCTTGAGTAAGTCTGCA;
oligonucleotide 2: 5′-TTACACATCCAGCCTCTGTGG;
oligonucleotide 3: 5′-CTTGGAGACATAGCCACACTG.

Pdx-1-Cre oligonucleotide up: 5′-ATGCTTCTGTCCGTTTGCCG;
oligonucleotide down: 5′-TGAGTGAACGAACCTGGTCG.

2.3 Histology

Tissues were fixed in 10% neutral buffered formalin (Sigma) for 24 h, dehydrated through a graded series of ethyl alcohol solutions and paraffin embedded. Pancreatic tissue was cut into 5-µm sections and stained with hematoxylin and eosin (H&E) for morphological assessment. Four non serial pancreatic sections were examined and images were acquired using a Nikon Eclipse E600 light microscope equipped with Olympus C-3030 digital camera.

2.4 *In vivo* and *ex vivo* BLI

For *in vivo* BLI, mice were anesthetized and 75 mg/kg of D-luciferin (Caliper, PerkinElmer company) was injected intraperitoneally. Ten minutes later, quantification of light emission was acquired for 5 minutes. Signal was detected using the IVIS Lumina II CCD camera system and analyzed with the Living Image 2.20 software package (Caliper Life Sciences). Photon emission was measured in specific regions of interest (ROIs). Data were expressed as photon/second/cm^2/steradiant (p/s/cm^2/sr). The intensity of bioluminescence was color-coded for imaging purposes; the scale used in each experiment is reported in each figure. For *ex vivo* BLI experiments, animals were sacrificed after *in vivo* BLI sessions and immediately subjected to a BLI session. Images of organs were detected as for the live animals.

3 Results and Discussion

3.1 Generation of bioluminescent PDAC mouse models.

It has been previously described a mouse model in which the expression of *Trp53*^{R172H}, concomitantly with that of *Kras*^{G12D}, leads to the development of invasive and metastatic PDAC that recapitulates clinical, histopathological, and genomic features of the cognate human disease (Hingorani et al., 2005). In order to visualize proliferation events during pancreatic tumour evolution we crossed these mice with the *MITO-Luc* mice that we recently described as a useful tool to track proliferation events *in vivo* in longitudinal studies in any body district. To this end, we first crossed *MITO-Luc* mice (FVB background) with *LSL-Kras*$^{G12D/+}$*;LSL-Trp53*$^{R172H/+}$ mice and with *Pdx-1-Cre* transgenic mice (C57Bl/6 background), respectively (Hingorani et al., 2005) To have a pure genetic background the mice were backcrossed into the FVB background for more than seven generations (Figure 1A). Next, the *MITO-Luc;LSL-Kras*$^{G12D/+}$*;LSL-Trp53*$^{R172H/+}$ genotype has been interbred with *MITO-Luc*;*Pdx-1-Cre* transgenic mice. Among the different genotypes depicted in figure 1B we focused our attention on *MITO-Luc;LSL-Kras*$^{G12D/+}$*;LSL-Trp53*$^{R172H/+}$*;Pdx-1-Cre* (MKPC) and *MITO-Luc;LSL-Kras*$^{G12D/+}$*;Pdx-1-Cre* (MKC). By specific PCR, the presence of the transgenes was assessed in the tail DNA (Figure 1C).

3.2 PDAC frequency and histological features of pre-invasive and invasive pancreatic lesions in FVB-based mouse models.

In MKPC mice in the FVB strain the prevalence of PDAC was 58,3% at 16 weeks of age and earliest tumour onset was histologically documented at 6 weeks of age, while in MKC mice the prevalence of PDAC was 16,6% at 16 weeks of age and earliest tumour onset was histologically documented at 11 weeks of age. Thus, MKPC mice have a reduced tumour-free survival, which is consistent with the reduced lifespan of KPC compared with KC mice described in the literature (median survival time of 203 for KPC vs 336 days for KC mice) (Hingorani et al., 2005; Cappello et al., 2013). Of note, none of the *MITO-Luc; Pdx-1-Cre* (MC) control mice developed tumours

(Table I). From a morphological point of view, MKPC and MKC mice developed pre-invasive and invasive ductal pancreatic cancer with the same histological features as those described for KPC and KC mice (Hingorani et al., 2003; Hingorani et al., 2005). In particular, the pancreas of MKPC and MKC mice developed PanIN lesions with complete penetrance. In fact, these ductal lesions were recognized in all the MKPC and MKC mice analysed, with or without an associated PDAC. Finally, PDAC developed in both MKPC and MKC mice showed a variable degree of differentiation, from well differentiated to undifferentiated. Representative examples of the invasive ductal adenocarcinoma seen in these animals are shown in figure 2 (Panels A-L). In contrast, no pre-invasive or invasive ductal lesions were observed in pancreas from age-matched control mice (MC) (Figure 2, panel M).

Taken together the *MITO-Luc* transgenic cassette does not influence the PDAC development already described in KPC and KC mouse models (Hingorani et al., 2005).

3.3 Longitudinal monitoring of PDAC-associated proliferation by *in vivo* and *ex vivo* BLI and its correlation with histopathology.

Next, we asked whether bioluminescent emission associated with tissue proliferation could be useful to identify early and/or premalignant stages of pancreatic cancer development. For this purpose MKPC and MKC were subjected to longitudinal *in vivo* imaging sessions starting at 6 weeks of age for several weeks until detection of a palpable tumour. Representative examples of MKPC mice developing tumours at 11 and 16 weeks of age respectively are shown in figure 3A. Of note, in these mice significant induction of abdominal luminescence was already observed one week before the palpable tumour could be detected indicating that imaging proliferation in these mice may allow an early detection of pancreatic cancer progression. In figure 3B are shown two examples of MKC mice, one developing tumour at 11 weeks of age (mouse # 355) and the other who did not develop cancer even at 23 weeks of age (mouse # 180). In the first mouse abdominal bioluminescence was observed one week before the palpable tumour was detected as well as at the

week in which the tumour was palpable. In contrast, no induction of abdominal luminescence was observed in pancreas from the MKC mouse that did not develop cancer (Figure 3B) and in MC control mice of any age (Supplementary Figure 1). *In vivo* imaging is carried out in two dimensions; thus the definition of the organ/tissue contributing to the photon emission is limited. To confirm the origin of the photon emissions from MKPC and MKC, the mice were sacrificed when the tumour became palpable and the gastrointestinal apparatus was subjected to *ex vivo* imaging. Examples of this analysis, shown in figure 3C, demonstrate that specific spots of BLI signals, although to a different extent, are emitted by the pancreatic mass in both mouse models. Interestingly, at 16 weeks of age bioluminescence signals from pancreas of MKPC mice were more intense than those from pancreas of MKC mice. Although in these experiments we did not reach a statistically significant sample size and further experiments are necessary to confirm this issue, these preliminary results are in agreement with our previous data demonstrating a crosstalk between mutant forms of *p53* protein and NF-Y that sustain an aberrant proliferation in cancer cells (Di Agostino et al., 2006). Moreover, the more intense *ex vivo* BLI signals observed in MKPC vs MKC mice were found to be positively associated with the presence of PDAC, which was histologically detected more often in the former transgenic model (Table II). As expected the bioluminescence signals are not present in the gastrointestinal apparatus from MC mice.

Altogether, *in vivo* and *ex vivo* analyses demonstrate that MKPC and MKC mouse models are powerful tools for visualizing PDAC development in terms of proliferation in the entire living animal in a *spatio*-temporal manner. Most notably, these results also demonstrate that in these mouse models it is possible to identify, non-invasively in living animals, early steps of pancreatic carcinogenesis in which proliferation events take place before tumour appearance. From a pharmacological point of view, this opens the possibility to design therapeutic protocols with a more precise timing than those using as a starting point the tumour palpability, a parameter of low specificity and sensitivity. Moreover, BLI technique is considerable more user friendly and less expensive than other *in vivo* imaging techniques such as MRI. Finally, from an ethical point of

view, application of BLI technique offers interesting additive values, too. Indeed, the analysis is carried out on the same living animal with a series of imaging sessions comfortable for the subject. Most important, this technique allows longitudinal experiments without sacrificing groups of mice at each time point thus reducing the necessary number of animals.

4 References

Capello, M.,Cappello, P., Linty, F.C., Chiarle, R., Sperduti, I., Novarino, A., Salacone, P., Mandili, G., Naccarati, A., Sacerdote, C., Beghelli, S., Bersani, S., Barbi, S., Bassi, C., Scarpa, A., Nisticò, P., Giovarelli, M., Vineis, P., Milella, M., Novelli, F., 2013. Autoantibodies to Ezrin are an early sign of pancreatic cancer in humans and in genetically engineered mouse models. J. Hematol. Oncol. 6, 67-79.

Cappello, P., Rolla, S., Chiarle, R., Principe, M., Cavallo, F., Perconti, G., Feo, S., Giovarelli, M., Novelli, F., 2013. Vaccination with ENO1 DNA prolongs survival of genetically engineered mice with pancreatic cancer. Gastroenterology. 144, 1098-106.

Cappello, P., Novelli, F., 2013. A self antigen reopens the games in pancreatic cancer. Oncoimmunology. 1, e24384.

Di Agostino, S., Strano, S., Emiliozzi, V., Zerbini, V., Mottolese, M., Sacchi, A., Blandino, G., Piaggio, G., 2006. Gain of function of mutant p53: the mutant p53/NF-Y protein complex reveals an aberrant transcriptional mechanism of cell cycle regulation. Cancer Cell. 10, 191–202.

Farina, A., Manni, I., Fontemaggi, G., Tiainen, M., Cenciarelli, C., Bellorini, M., Mantovani, R., Sacchi, A., Piaggio, G., 1999. Down-regulation of cyclin B1 gene transcription in terminally differentiated skeletal muscle cells is associated with loss of functional CCAAT-binding NF-Y complex. Oncogene. 18, 2818–2827.

Goeman, F., Manni, I., Artuso, S., Ramachandran, B., Toietta, G., Bossi, G., Rando, G., Cencioni, C., Germoni, S., Straino, S., Capogrossi, M., Bacchetti, S., Maggi, A., Sacchi, A., Ciana, P., Piaggio, G., 2012. Molecular imaging of nuclear factor-Y transcriptional activity maps proliferation sites in live animals. Mol. Biol. Cell. 23, 1467-74.

Gurtner, A., Manni, I., Fuschi, P., Mantovani, R., Guadagni, F., Sacchi, A., Piaggio, G., 2003. Requirement for down-regulation of the CCAAT-binding activity of the NF-Y transcription factor during skeletal muscle differentiation. Mol. Biol. Cell. 14, 2706–2715.

Gurtner, A., Fuschi, P., Magi, F., Colussi, C., Gaetano, C., Dobbelstein, M., Sacchi, A., Piaggio, G., 2008. NF-Y dependent epigenetic modifications discriminate between proliferating and postmitotic tissue. PLoS One. 3, e2047.

Gurtner, A., Fuschi, P., Martelli, F., Manni, I., Artuso, S., Simonte, G., Ambrosino, V., Antonini, A., Folgiero, V., Falcioni, R., Sacchi, A., Piaggio, G., 2010. Transcription factor NF-Y induces apoptosis in cells expressing wild-type p53 through E2F1 upregulation and p53 activation. Cancer Res. 70, 9711–9720.

Hidalgo, M., 2012. New insights into pancreatic cancer biology. Ann. Oncol. 23 Suppl. 10, x135-8.

Hingorani, S.R., Petricoin, E.F., Maitra, A., Rajapakse, V., King, C., Jacobetz, M.A., Ross, S., Conrads, T.P., Veenstra, T.D., Hitt, B.A., Kawaguchi, Y., Johann, D., Liotta, L.A., Crawford, H.C., Putt, M.E., Jacks, T., Wright, C.V., Hruban, R.H., Lowy, A.M., Tuveson, D.A., 2003. Preinvasive and invasive ductal pancreatic cancer and its early detection in the mouse. Cancer Cell. 4, 437–50.

Hingorani, S.R., Wang, L., Multani, A.S., Combs, C., Deramaudt, T.B., Hruban, R.H., Rustgi, A.K., Chang, S., Tuveson, D.A., 2005. $Trp53^{R172H}$ and $Kras^{G12D}$ cooperate to promote chromosomal instability and widelymetastatic pancreatic ductal adenocarcinoma in mice. Cancer Cell. 7, 469-83.

Hezel, A.F., Kimmelman, A.C., Stanger, B.Z., Bardeesy, N., Depinho, R.A., 2006. Genetics and biology of pancreatic ductal adenocarcinoma. Genes Dev. 15, 1218-49.

Manni, I., Mazzaro, G., Gurtner, A., Mantovani, R., Haugwitz, U., Krause, K., Engeland, K., Sacchi, A., Soddu, S., Piaggio, G., 2001. NF-Y mediates the transcriptional inhibition of the cyclin B1, cyclin B2, and cdc25C promoters upon induced G2 arrest. J. Biol. Chem. 276, 5570–5576.

Manni, I., Caretti, G., Artuso, S., Gurtner, A., Emiliozzi, V., Sacchi, A., Mantovani, R., Piaggio, G., 2008. Posttranslational regulation of NF-YA modulates NF-Y transcriptional activity. Mol. Biol. Cell. 19, 5203–5213.

Oliva, P., Roncoroni, C., Radaelli, E., Brunialti, E., Rizzi, N., De Maglie, M., Scanziani, E., Piaggio, G., Ciana, P., Komm, B., Maggi, A. 2013. Global profiling of TSEC proliferative potential by the use of a reporter mouse for proliferation. Reprod. Sci. 20, 119-28.

Rizzi, N., Manni, I., Vantaggiato, C., Delledonne, G.A., Gentileschi, M.P., Maggi, A., Piaggio, G., Ciana, P., 2015. In vivo imaging of cell proliferation for a dynamic, whole body, analysis of undesired drug effects. Toxicol. Sci. 145,296-306.

Sciortino, S., Gurtner, A., Manni, I., Fontemaggi, G., Dey, A., Sacchi, A., Ozato, K., Piaggio, G., 2001. The cyclin B1 gene is actively transcribed during mitosis in HeLa cells. EMBO. Rep 2, 1018–1023.

Signore, A., Mather, S.J., Piaggio, G.,Malviya, G., Dierckx, R.A., 2010. Molecular imaging of inflammation/infection: nuclear medicine and optical imaging agents and methods. Chem. Rev. 110:3112-45.

Spallotta, F., Cencioni, C., Straino, S., Nanni, S., Rosati, J., Artuso, S., Manni, I.,Colussi, C., Piaggio, G., Martelli, F., Valente, S., Mai, A., Capogrossi, M.C., Farsetti, A., Gaetano, C., 2013. A nitric oxide-dependent cross-talk between class I and III histone deacetylases accelerates skin repair. J. Biol. Chem. 288:11004-12.

Tuveson, D.A., Hingorani, S.R., 2005. Ductal pancreatic cancer in humans and mice. Cold Spring Harbor Symp. Quant. Biol. 70, 65-72.

Tuveson, D., Hanahan, D., 2011. Translational medicine: Cancer lessons from mice to humans. Nature. 471, 316–7.

Acknowledgements

We thank Daniela Bona for secretarial assistance, Cinzia Cataldo for technical assistance in histology processing and the Regina Elena Institute animal house (SAFU) for mouse breeding. This work has been partially supported by Italian Association for Cancer Research (AIRC) (IG-2012 n. IG13234) and Cariplo Foundation 2009-2439 to G.P.; Ministero della Sanità,-Progetti Ricerca Sanitaria Finalizzata (RF-2013-02354892 to F.N.), Associazione Italiana Ricerca sul Cancro (5 x mille no. 12182) and (IG no. 15257) to F.N.; University of Turin-Progetti di Ateneo 2011 (grant Rethe-ORTO11RKTW) and Progetto Progetti Ateneo 2014-Compagnia di San Paolo (PC-METAIMMUNOTHER to F.N and P.C.); PANTHER. to P.C; Sapienza University of Rome ("Progetto Ateneo 2013") to S.M; IRE internal projects to G.L.G.

We are indebted to Dr Silvia Bacchetti, McMaster University, Hamilton, Canada for critical reading of the manuscript and for the helpful and stimulating discussions.

Figure Legend

Fig. 1. ***Genetic strategy for generation of bioluminescent pancreatic ductal adenocarcinoma mouse models.*** (**A**): Schematic representation of different genotype transgenic mice obtained from *MITO-Luc* mice (FVB background) crossed with *LSL-Kras*$^{G12D/+}$*;LSL-Trp53*$^{R172H/+}$ mice (C57Bl/6 background) and *MITO-Luc* mice (FVB background) crossed with with *Pdx-1-Cre* mice (C57Bl/6 background). To obtain a pure genetic background mice were backcrossed into the FVB background for more than seven generations. In gray are indicated the genotypes used for the crossing in B. (**B**) Schematic representation of different genotype transgenic mice obtained from *MITO-Luc;LSL-Kras*$^{G12D/+}$*;LSL-Trp53*$^{R172H/+}$ mice crossed with *MITO-Luc;Pdx-1-Cre* mice. In gray genotypes used in the experiments described in this paper. (**C**) PCR of tail DNA from 1-month-old mice, *MITO-Luc;LSL-Kras*$^{G12D/+}$*;LSL-Trp*$^{H172R/+}$*;Pdx-1-Cre* and *MITO-Luc*;*LSL-KRAS*$^{G12D/+}$*;Pdx-1-Cre* mice. The bands represent the presence of the indicated cassettes. PCR products were separated on a 2% agarose gel. Molecular weight markers (1Kb Plus DNA Ladder, Invitrogen) was in the last lane from left.

Fig. 2. ***Histological appearance of invasive pancreatic ductal adenocarcinoma (PDAC) in FVB based MKPC and MKC mice.***

Hematoxylin and eosin (H&E) staining of pancreas sections from 11 week old MKPC and MKC mice. (**A** and **C**) PanINs (boxes) at the junction between normal acini (asterisks) and invasive PDA in MKPC (**A**) and MKC (**C**) mice (100X). (**B** and **D**) PanINs (arrows) at higher magnification in MKPC (**B**) and MKC (**D**) mice (250X). (**E-L**) Architectural features of invasive PDAC in MKPC (**E-G**) and MKC (**H-L**) mice (250X). (**E** and **H**) well-differentiated regions of PDAC showing prominent glandular and acinar architecture in MKPC (**E**) and MKC (**H**) mice; (**F** and **I**) regions of poorly differentiated PDAC in MKPC (**F**) and MKC (**I**) mice; (**G** and **J**) tumour with predominant sarcomatoid differentiation (spindle cell type) in MKPC (**G**) and MKC (**J**) mice. (**K**) MC mice pancreas shows normal cuboidal ductal epithelium (arrows), islet of Langherans (IL), and surrounding acinar tissue (250X).

Fig. 3. ***Longitudinal monitoring of PDAC associated proliferation by in vivo and ex vivo BLI.***

In vivo BLI of two MKPC (**A**) and two MKC (**B**) representative mice respectively, at the indicated weeks. The images were collected from 13 MKPC and 17 MKC mice, respectively; two representative animals per group are shown. (**A**) The two MKPC mice developed tumours at 11 and 16 weeks old, respectively. (**B**) One of the two MKC mice developed tumours at 11 weeks of age while the other did not develop tumour until 23 weeks. (**C**) *Ex vivo* BLI of pancreas from MKPC, MKC and MC mice. After the animals were sacrificed, the pancreas were collected at the indicated weeks of age. Images of five animals for each genotype were collected and one representative animal is shown. Both in A and B light emitted from the animal appears in pseudocolor scaling.

SFig1. BLI of a representative MC control mice from 7 weeks of age until 23 week of age. No induction of abdominal luminescence was observed in pancreas from the MC mice.

Table I

PDAC prevalence in MKPC, MKC and MC mice at 6, 11 and 16 weeks of age. MKPC = *MITO-Luc;LSL-Kras$^{G12D/+}$;LSL-Trp53$^{R172H/+}$;Pdx-1-Cre*; MKC = *MITO-Luc;LSL-Kras$^{G12D/+}$;Pdx-1-Cre*; MC = *MITO-Luc;Pdx-1-Cre*; PanINs = Pancreatic Intraepithelial Neoplasia; PDAC = pancreatic ductal adenocarcinoma; n. d. = not detected.

Table II

Histopatology and *ex vivo* BLI signal quantification (p/s/cm^2/sr) in MKPC, MKC and MC mice. MKPC = *MITO-Luc;LSL-Kras$^{G12D/+}$;LSL-Trp53$^{R172H/+}$;Pdx-1-Cre*; MKC = *MITO-Luc;LSL-Kras$^{G12D/+}$;Pdx-1-Cre*; MC = *MITO-Luc;Pdx-1-Cre*; PDAC = pancreatic ductal adenocarcinoma.

TABELLA 1

Genotype	PDAC 6^ week	PDAC 11^ week	PDAC 16^ week	% PDAC 6^ week	% PDAC 11^ week	% PDAC 16^ week	earliest tumor of uptake
MPKC	2/24	5/16	7/12	8.33%	31.25%	58.33%	6^ week
MKC	0/21	1/21	2/12	0%	4.76%	16.66%	11^ week
MC	0/17	0/14	0/9	0%	0%	0%	-

TABELLA 2

MKPC	Week old	Histopathology	Avg Radiance (p/s/cm^2/sr)
1	6	PanINs grade 1-A and 1-B	6,40E+05
2	6	PDAC, well differentiated	8,64E+05
3	8	PDAC, well and poorly differentiated regions	9,54E+06
4	8	PDAC, well differentiated	8,54E+05
5	11	PDAC, poorly differentiated	5,02E+06
6	11	PDAC, well differentiated	1,83E+06
7	16	PDAC, poorly differentiated	3,93E+07
MKC	**Week old**	**Histopathology**	**Avg Radiance (p/s/cm^2/sr)**
1	11	PanINs grade 1-A and 1-B; rare PanINs grade 2-3	2,08E+06
2	11	PanINs grade 1-A and 1-B	3,14E+06
3	11	PDAC, well differentiated	2,24E+06
4	11	PanINs grade 1-A and 1-B	n.d.
5	11	rare PanINs grade 1-A and 1-B	n.d.
6	11	PanINs grade 1-A and 1-B	n.d.
7	11	rare PanINs grade 1-A	n.d.
8	11	PanINs grade 1-A and 1-B , rare PanINs grade 2-3	n.d.
9	14	PanINs 1-A and 1-B grade	7,67E+05
10	14	early PDAC, well differentiated	7,19E+05
11	16	PanINs 1-A and 1-B grade	n.d.
12	17	PanINs grade 1-A and 1-B , rare grade PanINs 2-3	n.d.
MC	**Week old**	**Histopathology**	**Avg Radiance (p/s/cm^2/sr)**
1	6	normal pancreatic tissue, no PanINs	n.d.
2	8	normal pancreatic tissue, no PanINs	3,27E+05
3	8	normal pancreatic tissue, no PanINs	6,58E+05
4	11	normal pancreatic tissue, no PanINs	4,25E+05
5	11	normal pancreatic tissue, no PanINs	n.d.
6	11	normal pancreatic tissue, no PanINs	n.d.
7	16	normal pancreatic tissue, no PanINs	2,95E+05

FIGURA 1

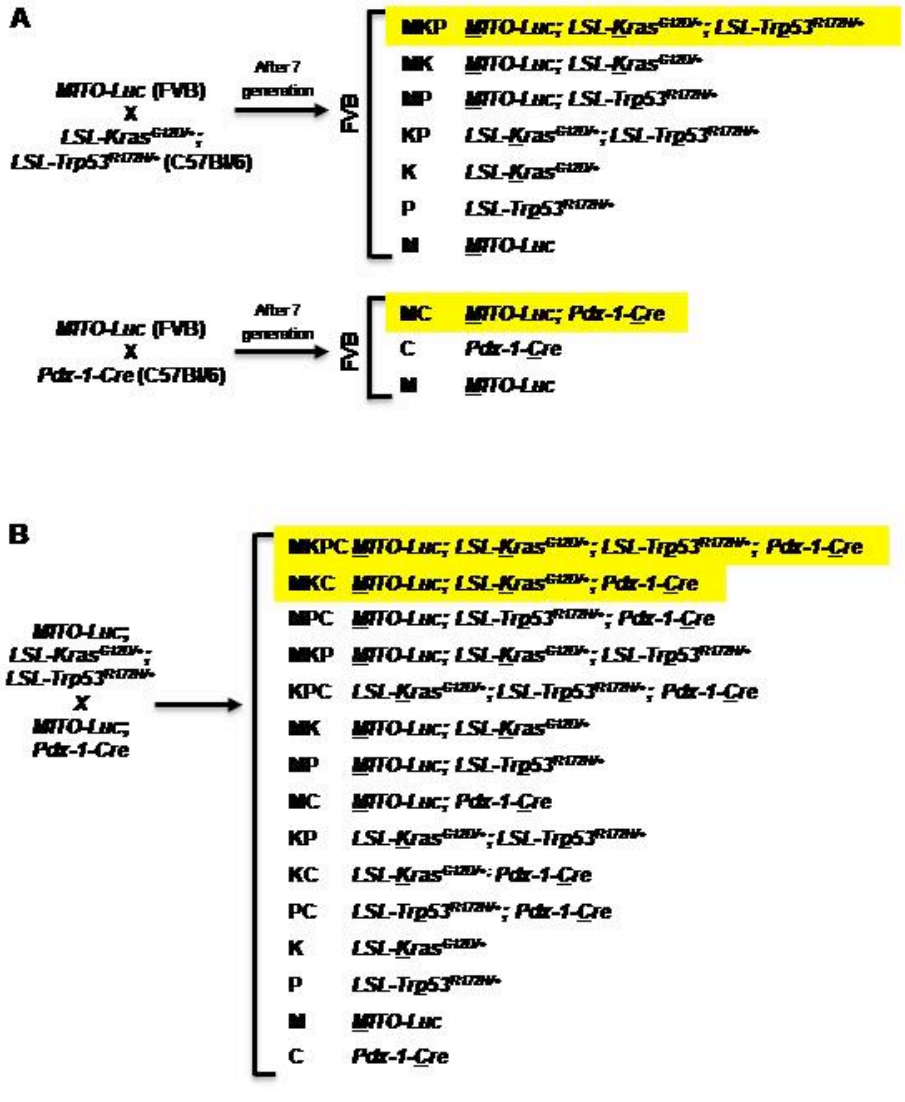
A
MITO-Luc (FVB)
X
LSL-KrasG12D/+;
LSL-Trp53R172H/+ (C57BL/6)
After 7 generation
FVB
MKP MITO-Luc; LSL-KrasG12D/+; LSL-Trp53R172H/+
MK MITO-Luc; LSL-KrasG12D/+
MP MITO-Luc; LSL-Trp53R172H/+
KP LSL-KrasG12D/+; LSL-Trp53R172H/+
K LSL-KrasG12D/+
P LSL-Trp53R172H/+
M MITO-Luc
MITO-Luc (FVB)
X
Pdx-1-Cre (C57BL/6)
After 7 generation
FVB
MC MITO-Luc; Pdx-1-Cre
C Pdx-1-Cre
M MITO-Luc
B
MITO-Luc;
LSL-KrasG12D/+;
LSL-Trp53R172H/+
X
MITO-Luc;
Pdx-1-Cre
MKPC MITO-Luc; LSL-KrasG12D/+; LSL-Trp53R172H/+; Pdx-1-Cre
MKC MITO-Luc; LSL-KrasG12D/+; Pdx-1-Cre
MPC MITO-Luc; LSL-Trp53R172H/+; Pdx-1-Cre
MKP MITO-Luc; LSL-KrasG12D/+; LSL-Trp53R172H/+
KPC LSL-KrasG12D/+; LSL-Trp53R172H/+; Pdx-1-Cre
MK MITO-Luc; LSL-KrasG12D/+
MP MITO-Luc; LSL-Trp53R172H/+
MC MITO-Luc; Pdx-1-Cre
KP LSL-KrasG12D/+; LSL-Trp53R172H/+
KC LSL-KrasG12D/+; Pdx-1-Cre
PC LSL-Trp53R172H/+; Pdx-1-Cre
K LSL-KrasG12D/+
P LSL-Trp53R172H/+
M MITO-Luc
C Pdx-1-Cre
C
MITO Kras Trp53 Cre M
MKPC
MITO Kras Cre M
MKC

FIGURA 2

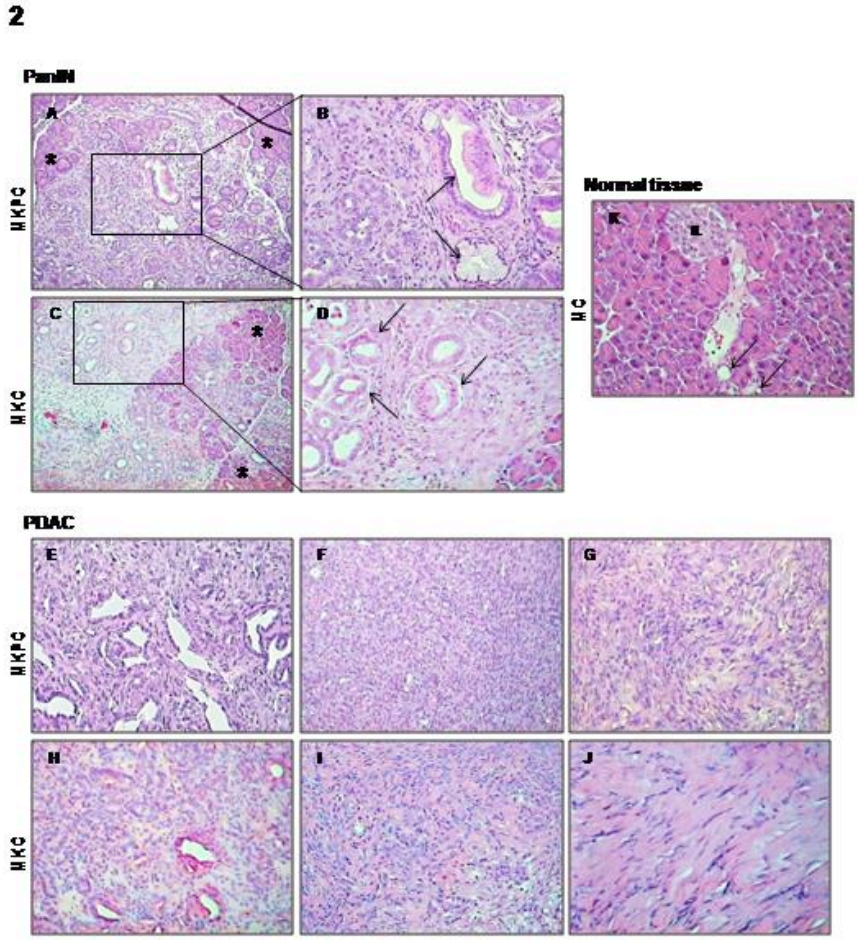

FIGURA 3

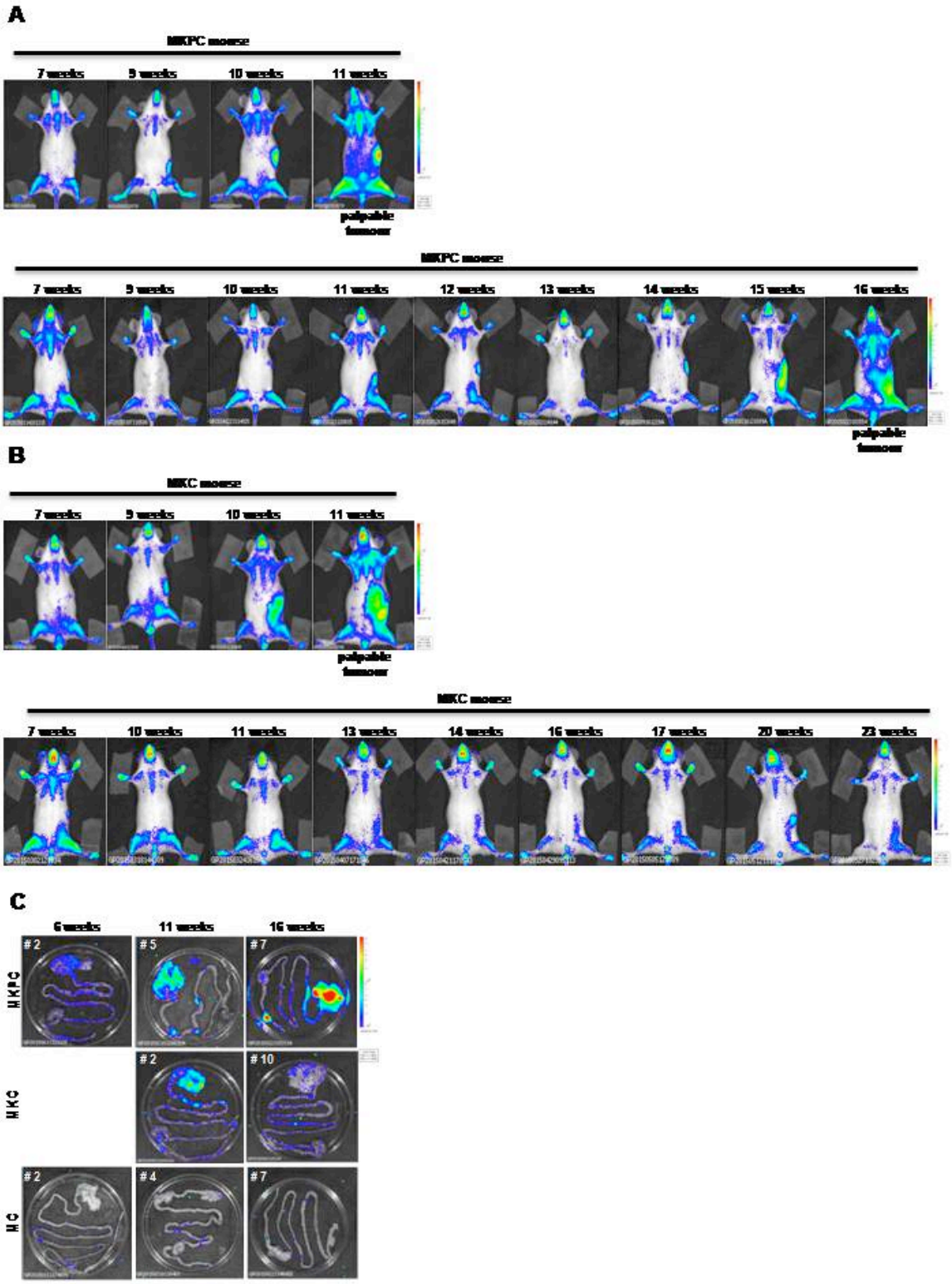
A
MKPC mouse
7 weeks
9 weeks
10 weeks
11 weeks
palpable tumour
MKPC mouse
7 weeks
9 weeks
10 weeks
11 weeks
12 weeks
13 weeks
14 weeks
15 weeks
16 weeks
palpable tumour
B
MKC mouse
7 weeks
9 weeks
10 weeks
11 weeks
palpable tumour
MKC mouse
7 weeks
10 weeks
11 weeks
13 weeks
14 weeks
16 weeks
17 weeks
20 weeks
23 weeks
C
6 weeks
11 weeks
16 weeks
MKPC
#2
#5
#7
MKC
#2
#10
MC
#2
#4
#7

SUPPLEMENTARY FIGURE 1